White beam differential phase and dark field imaging at high resolution

M Endrizzi[1*], GK Kallon[1], L Brombal[2,3], R Longo[2,3], N Sodini[4], D Dreossi[4], A Olivo[1]

[1.] Department of Medical Physics and Biomedical Engineering, University College London, Gower Street, London WC1E 6BT, United Kingdom
[2.] Dipartimento di Fisica, Università degli Studi di Trieste, Via A. Valerio 2, 34127 Trieste, Italy
[3.] Istituto Nazionale di Fisica Nucleare, Sezione di Trieste, Via A. Valerio, 2, 34127 Trieste, Italy
[4.] Sincrotrone Trieste SCpA, S.S. 14 km 163.5, 34012 Basovizza Trieste, Italy
* m.endrizzi@ucl.ac.uk

X-ray phase-contrast imaging (XPCI) can extend the capabilities of conventional radiography and, by exploiting phase effects, make visible those details that lack enough absorption contrast [1]. Several approaches have been proposed for XPCI by using synchrotron radiation, microfocal and extended labortory sources [2]. We focus here on edge illumination [3] in view of its properties of high resolution, sensitivity, robustness and achromaticity [4-6]. The latter is of particular interest for the study reported here, where we used the direct beam from a bending magnet, aiming at making use of a spectral distribution as broad as possible.

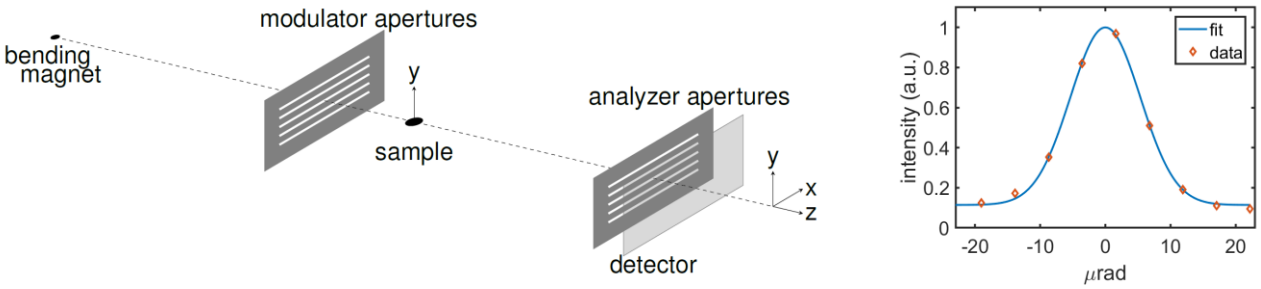

Figure. 1. Sketch of the experimental setup, the white beam from bending magnet is amplitude-modulated before it reaches the sample and it is analyzed by a set of aperture before detection. The experimental illumination function of such a system is reported in the panel on the right-hand side.

The experiment is sketched in Figure 1. The white beam from a bending magnet source is structured by a set of horizontal apertures that modulate the beam amplitude. After traversing the sample, the beam propagates until it reaches another set of apertures that serve as an analyzer placed immediately before the detector. Both the modulator and the analyzer are made of gold septa, with 20 μm pitch and 3 μm apertures. The detected intensity changes as a function of the vertical misalignment between the two sets of apertures. This is described by the (IF) illumination function $L(y)$, that can be conveniently expressed by the sum of Gaussian terms $L(y) = \sum_{n=1}^{N}(A_n/\sqrt{2\pi\sigma_n^2})\exp\left[-\frac{(y-\mu_n)^2}{2\sigma_n^2}\right]$ [7]. Once the object $O(y)$ is placed in the beam, the detected intensity can be written as

$$I(y) = \sum_{m=1}^{M}\sum_{n=1}^{N} A_{mn}\exp\left[-\frac{(y-\mu_{mn})^2}{2\sigma_{mn}^2}\right]$$

where $\mu_{mn} = \mu_m + \mu_n$, $\sigma_{mn}^2 = \sigma_m^2 + \sigma_n^2$ and $A_{mn} = A_m A_n(1/\sqrt{2\pi\sigma_{mn}^2})$; and the object function has also been expressed as series of Gaussian terms $O(y) = \sum_{m=1}^{M}(A_m/\sqrt{2\pi\sigma_m^2})\exp\left[-\frac{(y-\mu_m)^2}{2\sigma_m^2}\right]$. For this

experiment $N = 2$ terms were used for the illumination function and only $M = 1$ term was used for the object function. The field of view was limited by the detector size in the horizontal direction to about 6 mm, and by the beam size in the vertical direction to approximately 3.5 mm. Amplitude modulation requires that the sample is scanned in the vertical direction by sub-pitch displacements; we used 7 steps of 3 μm each for this experiment. We acquired 10 separate points for the IF, evenly spread to cover one pitch of the modulator. The intensity is analyzed pixel-by-pixel [8] and the contributions of the sample in terms of absorption, refraction and scattering are evaluated by means of a non-linear fitting procedure.

We imaged a bamboo wood sample as a test object. The retrieved images (transmission, refraction and dark-field) are shown separately in Figure 2. The spatial resolution is estimated to be around 3 μm. Details of the hierarchical microstructure of the wood sample are clearly distinguishable. Two horizontal bands, near the top and near the bottom of the images, exhibit substantially higher noise with respect to the central part of the images. This is due to a non-optimal sampling of the IF and subsequent instability of the retrieval procedure in those regions. Algorithms for the correction of these artefacts are being developed as well as the optimization of the data acquisition, which can be tuned to minimize those errors. Extension of the concepts presented here to three-dimensional imaging is underway [9].

References:

[1] R Fitzgerald, Physics Today **53** (2000), pp. 23-6.
[2] M Endrizzi, NIM A **878** (2018), pp. 88-98.
[3] A Olivo *et al*, Medical Physics **28** (2001), pp. 1610-19.
[4] M Endrizzi *et al*, Optics Letters **39** (2014), pp. 3332-5.
[5] M Endrizzi *et al*, Physical Review Letters **118** (2017), p. 243902.
[6] T Millard *et al*, Review of Scientific Instruments **84** (2013), p. 083702.
[7] M Endrizzi *et al*, Applied Physics Letters **104** (2014), p. 024106.
[8] M Endrizzi *et al*, Applied Physics Letters **107** (2015), p. 124103.

[9] M. E. was supported by the Royal Academy of Engineering under the RAEng Research Fellowships scheme. We thank Elettra Sincrotrone Trieste for access to SYRMEP beam line (Proposal No. 20170069) that contributed to the results presented here.

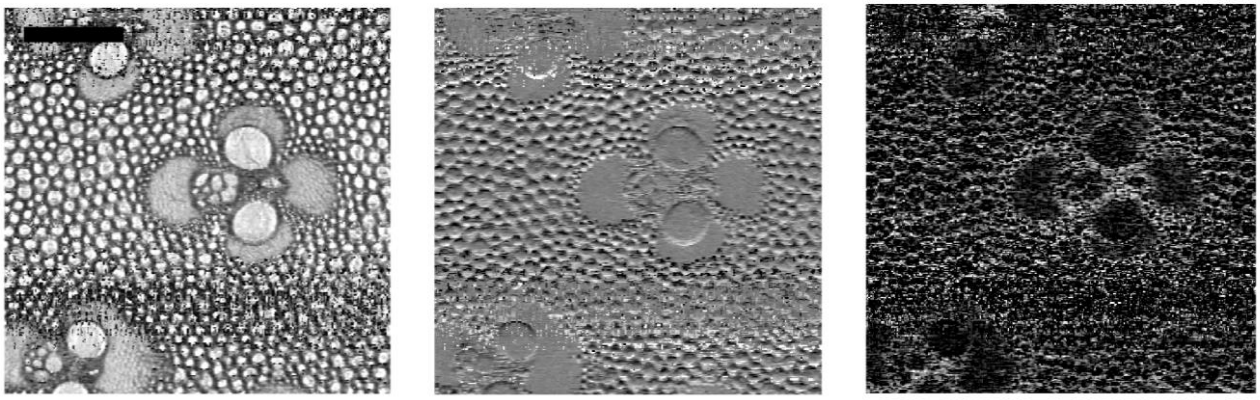

Figure. 2. Test images from a bamboo wood sample. From left to right: transmission, refraction and scattering representations of the sample. The scale bar in the top-left corner is 300 μm.